
Accuracy and microstructure of additively manufactured and post-machined parts

Hans-Christian Möhring, Dina Becker

Institute for Machine Tools - University of Stuttgart

hc.moehring@ifw.uni-stuttgart.de

Abstract

This contribution presents investigations regarding the accuracy and microstructure of additively manufactured specimens before and after post-machining. The additive manufacturing technology of laser metal wire deposition (LMWD) was applied for generating cylindrical test parts out of AlMg5 aluminium alloy. For that purpose, a specific laser power control strategy was implemented in order to achieve a stable material deposition at the thin-walled test structure. The test specimens were analysed with respect to the influence of the additive processing on the geometric properties and the microstructure as well as the porosity of the material. The specimens were subsequently machined by turning, and the influence of this post-processing on the properties of the test parts was analysed regarding the final shape accuracy as well as Martens hardness. The analyses revealed a clear dependence of the material properties on the layer structure that was built during additive manufacturing. The rough shape of the additively manufactured specimens has an influence on the cutting conditions during the post-machining process. These influences also affect the final properties of the additively and subtractively produced parts.

Accuracy, Cutting, 3D printing, Microstructure

1. Introduction

Additive processes offer the possibility for a near-net-shape production of components with locally adapted mechanical properties, which can be optimized by downstream process steps in accordance with the load [1]. However, additively manufactured components do generally not have the required dimensional accuracy and surface quality for functional surfaces such as flanges, guides, bearing seats, etc and therefore have to be reworked by machining operations in most cases [2]. However, this remachining required for the realisation of the necessary function-related geometry and surface accuracies interacts with the result of the additive process, making it indispensable to take both processes into account. Laser-based additive manufacturing processes such as laser cladding or selective laser melting (laser powder bed fusion - LPBF) are used to process metals in the form of powder or wire, achieving strengths comparable with those of conventionally manufactured components. In this way, higher surface qualities are achieved with the powder bed-based processes and graded component conditions. Moreover, the porosity can be adjusted by means of adapted process strategies. In contrast, higher deposition rates are achieved with build-up welding due to a significantly higher average convertible laser power of several kW, compared with only several hundred watts in powder bed-based processes. Although quality is an important factor, the deposition rate must be greatly increased to make AM processes competitive with conventional manufacturing processes by reducing production time. As already mentioned for build-up welding, this can be achieved by using filler materials such as wire. An AM process that also uses this filler metal is the laser metal wire deposition process (LMWD). In recent years, LMWD

has been improved to produce simple 3D-printed parts with low accuracy. Different strategies for 3D printing with wire were evaluated [3]. Aluminium as a filler wire material was also used in some studies to make simple cylindrical parts [4].

This study investigates the accuracy and microstructure of AlMg5 aluminium alloy specimens produced by a controlled LMWD process with subsequent subtractive machining by turning.

2. Test components, process and measurement set-up

The additively manufactured specimens (cylinders) were produced in cooperation with the Institute of Laser Technologies (IFSW) at the University of Stuttgart [5]. Fig. 1. shows the processing head, a schematic representation and the process itself. The production parameters were adapted to produce the most thin-walled cylinders as possible with a high surface quality to maximize the material usage for the post-processing operation. The laser power here was between 1200 and 2640 kW, the fibre diameter was 600 μm , the wavelength was 1030 nm and the track speed was 2 m/min. The cylinders were fabricated with a programmed diameter of 40 mm and a fixed number of layers up to a height of about 37 mm.

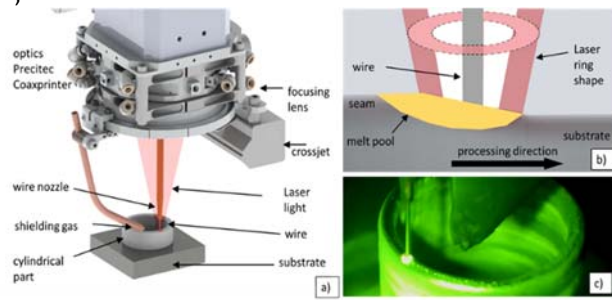


Figure 1. LMWD process: a) processing head; b) laser ring shape and wire; c) deposition process [6]

In order to keep the wall thickness as small as possible with a given AlMg5 wire ($D = 1\text{ mm}$) and to create the cylindrical shape as uniformly as possible, a small beam diameter (2.5 mm) was used. To reduce the wall thickness, the laser power of the LMWD process was reduced with the specimen height. The LMWD process was carried out using inert gas nitrogen with and without track height control by means of optical coherence tomography (OCT).

To produce the desired cylindrical nominal contour of the additively manufactured specimens, these were subsequently machined. The required external longitudinal turning operation was carried out with an R200 turning/milling centre by INDEX-Werke using water-based flood lubrication (Blasocut BC 935 K).

The additively manufactured cylindrical specimens were analysed with a 3D coordinate measuring machine, type MC850 by Carl Zeiss, using an ultrahigh-precision contact probe system with a measuring ball radius of 2.5 mm . The measuring strategy for the specimens was created with the Calypso software to measure the element from the outside and inside with a contact probe. The measuring distance along the additively built direction (Z-axis) was 1 mm .

The 2D roughness of the test specimens was examined with the Formtracer SV-C3200 contact measuring device.

To determine the macroscopic structure of the specimens, the samples were subjected to etching with a 10% NaOH solution heated to approx. 55°C . For this purpose, the samples were carefully separated by means of a cut-off wheel with interrupted cuts, then embedded, ground (grain size 240, 500, 1000, 2000 and 4000, pressure force 20-30 N) and finally polished with a diamond suspension.

The electrolytic etching process of Barker enables the creation of colour etchings in aluminium alloys. The investigated samples were embedded using a 2-component embedding agent based on highly cross-linked methyl methacrylate. Then they were ground up to a grain size of 4000 in steps of 320, 500, 800, 1000, 2500 and 4000. Finally, they were polished with a diamond suspension on a synthetic fibre plate ($3\text{ }\mu\text{m}$).

To determine the hardness, the indentation test was carried out according to DIN EN ISO 14577-1 and ASTM E 2546, using a Picodentor HM500. The Martens hardness (HM) is defined as the ratio of the maximum force to the corresponding contact area and is given in N/mm^2 .

3. Results and discussion

The produced specimen were evaluated after the additive LMWD process and after the machining process. For both processes, metallographic tests as well as hardness tests were investigated and presented.

3.1 Shape accuracy of the LMWD process

The test specimens were produced at decreasing laser power levels to ensure a stable and complete process. The process without track height control started at a high laser power of $2,500\text{ W}$ and ended at a laser power of $2,000\text{ W}$. During the process, the laser power was reduced twice: from $2,500\text{ W}$ to $2,250\text{ W}$ (between $2\text{--}3.5\text{ mm}$) and from $2,250$ to $2,000\text{ W}$ (between $8\text{--}12\text{ mm}$). Regarding the test specimens with OCT control, the laser power was diminished continuously from $2,500\text{ W}$ to $2,000$ during the LMWD process (Fig. 2).

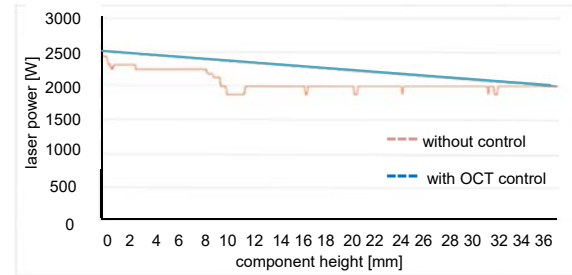


Figure 2. Laser power in the LMWD process

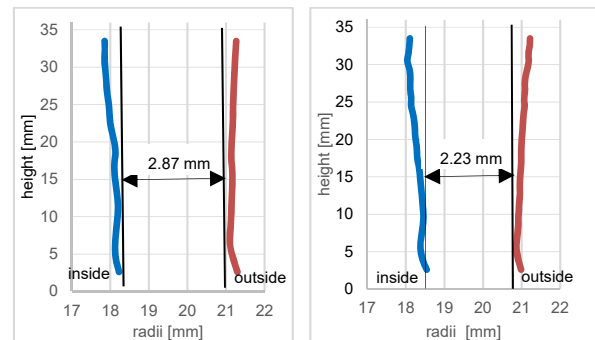


Figure 3. Examples of the wall thickness or outer and inner radii: a) process without control; b) with OCT control

The wall thickness of all test specimens increased because the heat accumulated in the upper part of the samples (Fig. 3). However in the process with OCT control, the homogeneous (effective) wall thickness of the test specimens was significantly thinner and amounted to 2.23 mm (2.87 mm without control). For the cylinder of the process without control, the thin (effective) wall thickness was between $10\text{--}12\text{ mm}$ component height and thus correlated with the great reduction of the laser power from $2,500$ to $2,000\text{ W}$ in the LMWD process. The cylinders of the OCT-controlled processes are thin at the beginning of the additive process but increase continuously with the cylinder height.

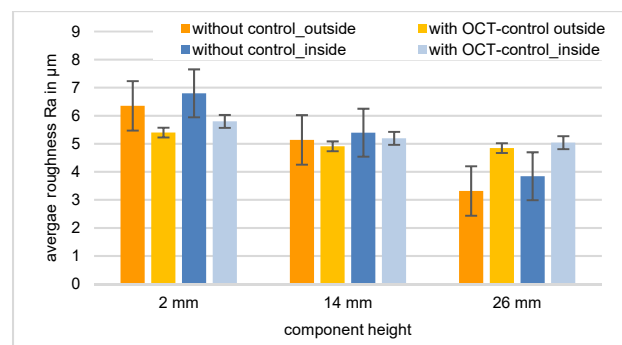


Figure 4. Roughness characteristics Ra on the outside and inside of the specimen

Subsequently, the 2D roughness of the test specimen was examined. The investigations were focussed on determining the characteristic values R_a for the evaluation of the surface quality of the LMWD components. Figure 4 clearly shows that the outer side of all the test specimens produced had R_a -values that were approx. 0.3 - 0.4 mm lower than those of the inner side. The roughness R_a decreased with the component height for all test specimens and reached $R_a = 3.32 \mu\text{m}$ (process without control) and $R_a = 4.84 \mu\text{m}$ (with OCT control) on the outside at 26 mm. In general, the R_a -values at the beginning of the LMWD process (component height of 2 mm) were approx. 1.9 times (process without control) and 1.1 times (process with OCT control) higher than for the component height of 26 mm.

3.2 Subtractive machining

To increase the dimensional accuracy of the test specimen, the specimen was turned from outside (Fig.5). In order to achieve the highest possible efficiency of the overall process, the volume of material to be used in the additive production phase should be as high as necessary and the volume of material to be removed should be kept as low as possible in the subtractive machining phase. The maximum dimensions of an ideal outside cylinder for the samples (best possible cylindricity) were derived from the measurements of the outer radii (Fig. 3). For this reason, the depth of cut was 0.15 mm (calculated starting from r_{min} on the outside), the feed rate was $f = 0.05 \text{ mm/revolution}$ and the cutting velocity was $v_c = 500 \text{ m/min}$. The removed metal amounted to 28.83 mm^3 (without control) and 30.21 mm^3 (with OCT control) of the complete material volume. Fig. 5 shows a typical LMWD test component from outside before and after turning.

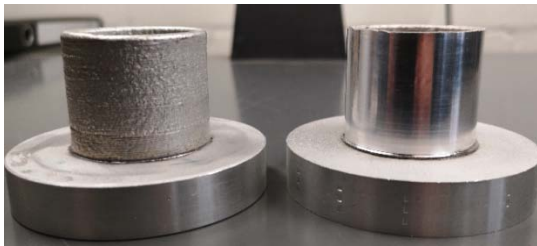


Figure 5. Typical test component before (left) and after the turning process (right).

Regardless of the type of additive process, the roughness values after machining hardly differed and were $R_a = 0.15 - 0.2 \mu\text{m}$ (Fig. 6). As expected, the R_a -values in the lower and upper part area were a little lower than in the middle of the part, as more material was removed there.

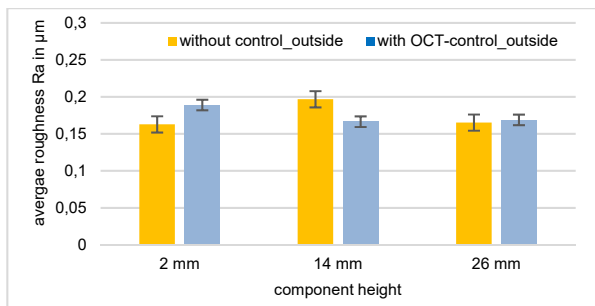


Figure 6. Roughness characteristics R_a on the outside after external longitudinal turning

3.3 Microstructure of additively manufactured and post-machined test components

For the examination of the internal structure of the test specimen, the metallographic sections were prepared. The prepared sections of the test specimen were examined macroscopically and compared with each other (Fig. 7). Analogously to the measured radii (Fig. 3), the layer width increased continuously over the component height for the LMWD process with and without track height control. However, the distance between the layers was different. For the process variant without control, there was a great distance of $750 - 803 \mu\text{m}$ between the layers deposited with the high laser power $2,500 - 2,250 \text{ W}$ (component height of $h = 0 - 8 \text{ mm}$). At a constant laser power of $2,000 \text{ W}$, the layer distance was reduced to $380 - 520 \mu\text{m}$ (component height of $h = 12 - 35 \text{ mm}$). In contrast, no distinct areas with a strongly differing distance between the layers could be found in the test specimens with OCT control. Over the component height, the layer distance varied between $620 - 370 \mu\text{m}$.



Figure 7. Etching of samples a) without control, b) with OCT control (NaOH etching). Cutting plane perpendicular to the feed direction

Another interesting aspect was to compare the components of the microstructure of the additively manufactured specimens without and with OCT control of the track height. The microstructure of the test specimen was evaluated in the middle of the wall of the cross-section according to the method proposed by Ohser and Lorz, by means of linear analysis using spatially random variables [6]. The points of intersection between the test lines and the grain boundaries were considered as random quantities. The test lines were made on a measuring surface of $0.572 \text{ mm} \times 0.431 \text{ mm}$. The distance between two individual vertical lines was $114.4 \mu\text{m}$ and $86.2 \mu\text{m}$ between parallel lines. The point density P_L of the intersections was calculated according to:

$$P_L = N/L \quad (1)$$

The test line length L is the sum of all L_x and L_y segments. N is the number of points of intersection. After the calculation, it was found that the intersection point density and thus the number of grains in the middle of the wall for LMWD samples with OCT control was 1.16 times higher than the intersection point density for samples without control, as can be deduced from Table 1. This indicated indirectly that there was a larger number or a greater compression of grains when the layers were deposited with control of the track height.

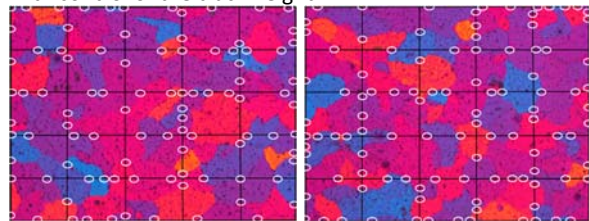


Figure 8. Sample cross-sections in the middle of the wall: process without control (left); with OCT control (right). x 200 magnification with exemplary points of intersection between the test lines and the grain boundaries for a component height of 21 mm, surface of $0.572 \text{ mm} \times 0.431 \text{ mm}$

For the test specimens with OCT control, the microstructure was examined at the outside of the test specimens before and after the turning process. It was found that the machined surfaces showed a significant reduction of scorch marks or pores in comparison with surface areas without machining operations (Fig. 9). The porous, brittle areas were removed during machining. In addition, plastic surface deformation occurred during machining, contributing to the closing of the pores by a filling effect.

Table 1. Exemplary Component of the microstructure (intersection point density)

LMWD process classification	line segment length [mm]	number of intersection points	intersection point density
without control of the track height	6.203	90	14.51
with control of the track height (OCT control)	6.203	105	16.93

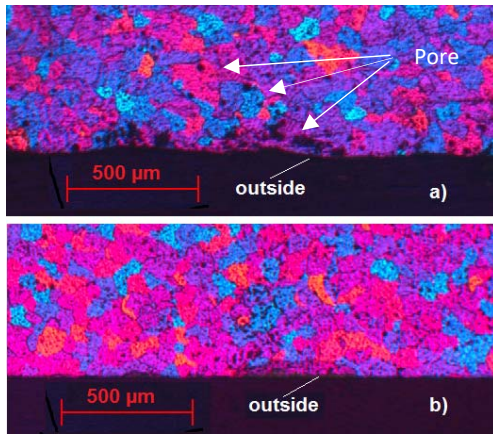


Figure 9. Microstructure of the component sides before (a) and after the turning process (b). x 25 magnification (sample with OCT control). Component height: 21-23 mm, depth of cut: 0.15 mm

Finally, the hardness of the test specimen was examined before and after longitudinal turning. The microhardness was analysed across the prepared microsections (component height of 21 - 22 mm). The measuring points were distributed in five areas. The first (outside) as well as the last area (inside) were approx. 50 µm away from the corresponding wall surface. The tests showed that the additively manufactured test specimens had a comparable hardness before machining. The maximum hardness of $HM = 750 - 760 \text{ N/mm}^2$ was determined in the centre of the wall specimen. After machining, both test specimens had higher hardness values at the turned side compared with the centre of the wall and at the unmachined side (inside). In the centre of the wall, the test specimens without control showed approx. 30 - 50 N/mm^2 higher HM values than the components with OCT control. Although the removed volumes of all test specimens were comparable, those without control had an approx. 0.5 mm greater wall thickness and therefore a higher heat capacity during machining than the thin test specimens from the process without OCT control. This could result in a grain compression in the following solidification.

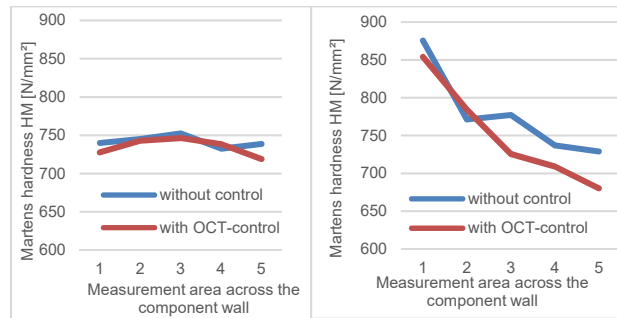


Figure 10. Influence of turning on hardness distribution in the wall cross-section before (left) and after (right) the turning process. Machining parameters: $vc = 500 \text{ m/min}$, $f = 0.05$; measurements of height: 21 - 22 mm

4. Summary

The heating during LMWD at reduced laser power had a strong effect on the wall thickness of the AlMg5 cylinder. By means of OCT-based track height control, cylinders with a wall thickness of 2.23 mm could be produced (2.87 mm without control). The OCT track height control led to a more constant distance between the layers and compression of the grains during the deposition process. By turning the additively produced specimens, it was possible to increase the specimen quality significantly. The porous, brittle areas were removed, and plastic deformation occurred on the machined surface. After the machining operation, the roughness characteristics along the height of the cylinder reached 0.16 - 0.19 µm (before machining: $R_a = 6.35 - 3.3 \text{ µm}$ for samples without control and $R_a = 5.38 - 4.88 \text{ µm}$ with OCT control $R_a = 5.38 - 4.88 \text{ µm}$). The hardness of the machined surface ($vc = 500 \text{ m/min}$, $f = 0.05 \text{ mm/revolution}$) was 12 % higher (without control) and 17 % higher (with OCT control) than in the middle of the component wall.

In future research, it is planned to investigate the influence of further types of LMWD control as well as different machining processes on the microstructure of LMWD components. The aim here will be to produce components with a great accuracy, defined surface roughness and defined values of hardness. Due to the LMWD process speed with high application rates and a material usage of almost 100 percent, the basic research as well as the planned investigations are to be most interesting for users from various industrial sectors.

References

- [1] Liu J. Y 2018 Current and future trends in topology optimization for additive manufacturing *Struct. Multidisc. Optim.* **57** 2457-83
- [2] Ding D., Pan Z., Cuiuri D. and Li H. Y 2015 Wire-feed additive manufacturing of metal components: technologies, developments and future interests *Int. J. Adv. Manuf. Technol.* **81** 465-81
- [3] Nowotny S. Y 2009 Laser-Präzisionsauftragsschweißen mit zentrischer Drahtzufuhr: BMBF-Rahmenkonzept "Forschung für die Produktion von morgen"; Ergebnisbericht zum Verbundvorhaben "Flexible 3D-Bearbeitung durch laserbasierte Fügeverfahren mit integrierter Werkstoffzufuhr" *Flexiglas*
- [4] Froend M., Riekehr S., Kashaev N., Klusemann B. and Enz J. Y. 2018 Process development for wire-based laser metal deposition of 5087 aluminium alloy by using fibre laser *Journal of Manufacturing Processes* **34** 721-32
- [5] Becker D, Boley S, Eisseler R, Stehle T, Möhring H-C, Onuseit V, Hoßfeld M, Graf T Y. 2021 Influence of a closed-loop controlled laser metal wire deposition process of S Al 5356 on the quality of manufactured parts before and after subsequent machining *Production Engineering* **15** 489-507
- [6] Ohser J. and Lorz U. Y. 1994 Quantitative Gefügeanalyse: Theoretische Grundlagen und Anwendungen 1. Aufl. *Freiberger Forschungshefte B Metallurgie und Werkstofftechnik*